

Description of two new *Labeo* (Labeoninae; Cyprinidae) endemic to the Lulua River in the Democratic Republic of Congo (Kasai ecoregion); a hotspot of fish diversity in the Congo basin

TOBIT L.D. LIYANDJA¹ AND MELANIE L.J. STIASSNY²

ABSTRACT

Labeo mbimbii, n. sp., and *Labeo manasseae*, n. sp., two small-bodied *Labeo* species, are described from the lower and middle reaches of the Lulua River (Kasai ecoregion, Congo basin) in the Democratic Republic of Congo. The two new species are members of the *L. forskalii* species group and are genetically distinct from all other species of that clade. Morphologically they can be distinguished from central African *L. forskalii* group congeners except *L. dhonti*, *L. lukulae*, *L. luluae*, *L. parvus*, *L. quadribarbis*, and *L. simpsoni* in the possession of 29 or fewer (vs. 30 or more) vertebrae and from those congeners by a wider interpectoral, among other features.

The two new species are endemic to the Lulua River and, although overlapping in geographical range and most meristic and morphometric measures, are readily differentiated by differing numbers of fully developed supraneural bones, predorsal vertebrae, snout morphology, and additional osteological features. The description of these two species brings the total of *Labeo* species endemic to the Lulua basin to three. The third endemic species, *L. luluae*, was previously known only from the juvenile holotype, but numerous additional specimens have now been identified. The cooccurrence of 14 *Labeo* species in the Lulua River, three of which are endemic, highlights this system as a hotspot of *Labeo* diversity in the Congo basin and across the continent.

¹ Richard Gilder Graduate School, American Museum of Natural History; Department of Ichthyology, American Museum of Natural History; and Département de Biologie, Faculté des Sciences, Université de Kinshasa, Kinshasa, Democratic Republic of Congo.

² Richard Gilder Graduate School, American Museum of Natural History; Department of Ichthyology, American Museum of Natural History.

INTRODUCTION

With 108 species currently recognized (Fricke et al., 2022; Froese and Pauly, 2022) *Labeo* is the second most diverse genus in the cyprinid subfamily Labeoninae, and is widely distributed throughout Africa and southeast Asia. The highest diversity is found in Africa and, based on morphometric and anatomical features, Reid (1985) divided the 80+ African *Labeo* into six species groups: *L. coubie* group, *L. forskalii* group, *L. gregorii* group, *L. macrostoma* group, *L. niloticus* group, and *L. umbratus* group. Among these the *L. forskalii* group is by far the most species rich and, with the exclusion of *L. alluaudi*, forms a monophyletic group (Lowenstein et al., 2011; Liyandja, 2018; Liyandja et al., 2022) comprising over a third of the species currently recognized in the Congo basin (Van Steenberge et al., 2016; Liyandja et al., 2022). However, because of widespread convergent morphological evolution, the taxonomy of many members of the *L. forskalii* group is problematical and remains a persistent impediment to sustainable resource management of these important fishes for subsistence fisheries (Liyandja et al., 2022).

A recent study (Mbimbi et al., 2021) has highlighted the Lulua River, a large right-bank tributary of the Kasai River (fig. 1), as harboring one of the most species-rich fish communities within the entire Congo basin. The Lulua basin is characterized by high geomorphological and hydrological complexity (Roberts et al., 2015) resulting in a wide range of disjunct habitats including numerous rapids and falls, pools, floodplains, and perennial and permanent swamps located within a dense river network of some 71,400 km² (Mbimbi et al., 2021). The Lulua ichthyofauna is rich in cyprinids, and most notable is the cooccurrence in the basin of an estimated 14 *Labeo* species (Mbimbi et al., 2021: table A2), rendering the river a potential hotspot of diversity for *Labeo* within the entire Congo basin. In a study of cryptic diversity within the *L. forskalii* group incorporating both morphological and molecular data, Liyandja et al. (2022) addressed some taxonomic issues highlighted by Mbimbi et al. (2021) but also recognized a number of undescribed lineages of *Labeo* represented among specimens from the Lulua basin and across central Africa. Despite the morphology-based revisionary works of Tshibwabwa (1997) and Reid (1985), the taxonomy and species limits of many of these *Labeo* remain problematical (Van Steenberge et al., 2016), and an integrative approach is necessary for better taxonomic resolution.

Liyandja et al. (2022) provided a necessary phylogenetic framework for taxonomic descriptions for the numerous previously unrecognized *L. forskalii* group members in central Africa. Here, in the first of a series of studies aimed at rectifying this taxonomic impediment, we integrate the results of the molecular phylogenetic analyses of Liyandja et al. (2022) with 2D geometric morphometrics, traditional linear measures, meristics, and osteological features to provide formal taxonomic descriptions for two new *Labeo* species; *L. mbimbii*, n. sp., and *L. manasseeae*, n. sp.

MATERIAL AND METHODS

SAMPLING AND PRESERVATION: Fishes were collected and euthanized in accordance with the guidelines for the use of fishes in research (Jenkins et al., 2014) and ethical considerations for field research (Bennett et al., 2016). The holotypes and some paratypes of the two new spe-

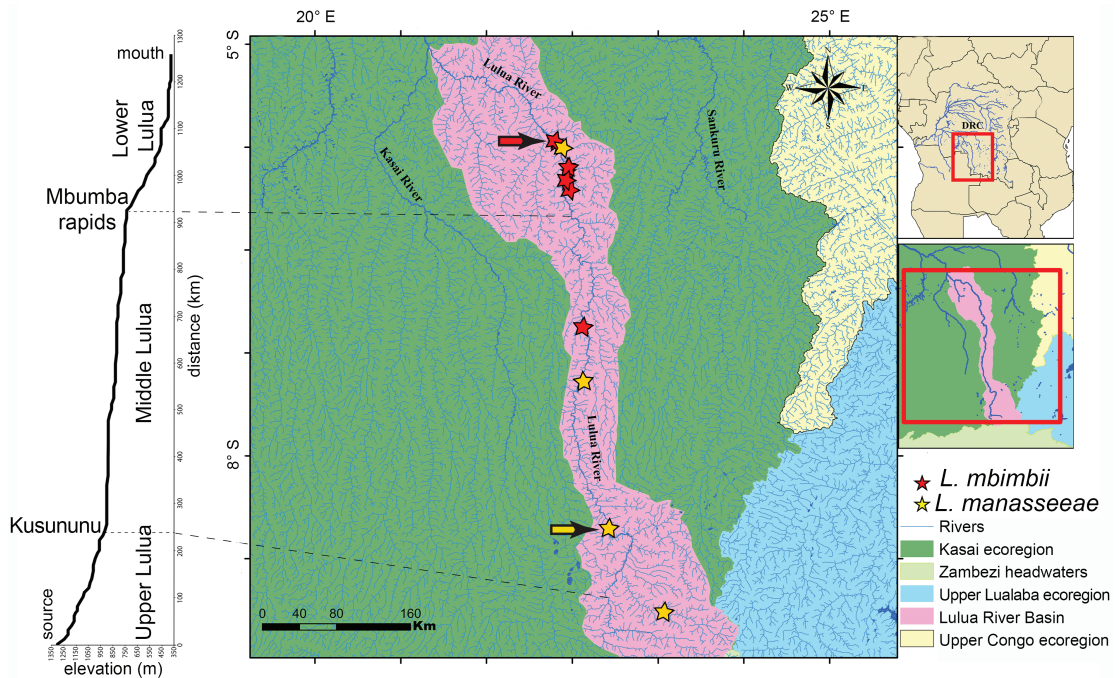


FIGURE 1. A. Longitudinal profile of the Lulua River indicating subdivision into three sections based on channel slope gradient (after Mbimbi et al., 2021). B. Lulua River basin showing collection localities of the two new species (arrows indicate type localities). C. Location of the Congo basin, Kasai, Lulua, and adjacent ecoregions.

cies were collected in the main channel of the Lulua River in September 2014. Topotypes of *L. lukulae* were collected during a 2018 expedition to the Lukula River (Lukula, Kongo Central, D.R.C.). All specimens were collected using gill-, cast-, and dip-netting techniques, and euthanized using MS-222. Samples were provisionally grouped to species using conspicuous morphological features and color patterns, photographed, and preserved in 10% formalin. Prior to preservation, fin clips were taken from 3 to 4 individuals per putative species and preserved in cryotubes containing 95% ethanol.

Additional voucher specimens and comparative materials were obtained from collections of the American Museum of Natural History (AMNH), the Academy of Natural Sciences of Drexel University (ANSP), Auburn University Museum of Natural History (AUM), the Bavarian State Collection of Zoology (ZSM), Cornell University Museum of Vertebrates (CUMV or CU), and Oregon State University Ichthyology Collection (OS). Other abbreviations are AMCC, Ambrose Monell Cryo Collection of the American Museum of Natural History; BD, body depth; CT, micro-CT scanned specimens; HL, head length; SL, standard length.

COMPARATIVE MATERIALS EXAMINED: A total of 120 specimens were included in our analyses. In addition to 32 specimens of the new species (26 *L. mbimbii*, n. sp., and 6 *L. manasseeae*, n. sp.), 88 other specimens were included (number of individuals examined in parenthesis): *L. annectens* (8); OS 20622 (1), OS 21441 (1), OS 21320 (6). *L. dhonti* (6); AMNH 271056 (4), CU 95264 (2). *L. lukulae* (16); AMNH 276342 (7 topotypes), AMNH 276343 (6 topotypes), AMNH

274961 (1), AMNH 274962 (1), ANSP 38553 (1). *L. luluae* (27); AMNH 243598 (9), AMNH 243599 (2), AMNH 247860 (3), AMNH 247970 (2), AMNH 247993 (2), AMNH 251177 (3), AMNH 253469 (1), AMNH 269106 (2), AMNH 269108 (2), ANSP 51740 (holotype). *L. parvus* (10); AMNH 276646 (1), AMNH 276647 (1), AMNH 278152 (1), CU 92141 (3 topotypes), CU 92147 (1 topotype), ZSM 42129 (3). *L. quadribarbis* (7); AMNH 253438 (1), AMNH 276667 (5), AUM 51572 (1). *L. simpsoni* (14); AMNH 240995 (2), AMNH 243589 (1), AMNH 247071 (3), AMNH 276658 (2), AMNH 276660 (1), AMNH 276663 (2), AUM 51572 (3).

MOLECULAR DATA COLLECTION AND ANALYSES: Genomic DNA was extracted from several individuals of *Labeo annectens*, *L. dhonti*, *L. lukulae*, *L. luluae*, *L. manasseae*, n. sp., *L. mbimbii*, n. sp., *L. parvus*, *L. polli*, *L. quadribarbis*, and *L. simpsoni* from the Congo basin and Lower Guinean ecoregions using the Qiagen Genra Puregene Tissue Kit following the manufacturers protocol. A portion (652 bp) of the cytochrome oxidase subunit 1 (COI) and the entire (1500 bp) recombination activate gene 1 (RAG1) were amplified and sequenced on a Sanger sequencing platform following the protocol of Lowenstein et al. (2011). Additional sequences were obtained from the Barcode of Life Data System (<http://www.barcodinglife.org>) and GenBank (www.ncbi.nlm.nih.gov/genbank). Phylogenetic analyses were conducted using both Bayesian inference (BI) and maximum likelihood (ML) as implemented respectively in MrBayes 3.2.2 (Ronquist et al., 2012) and IQ-TREE (Nguyen et al., 2015). For full details of molecular analytical methodology, see Liyandja et al. (2022).

MORPHOLOGICAL DATA COLLECTION AND ANALYSES: Specimens were photographed in ventral and lateral (left side) views using a mounted Canon EOS 600D digital camera. Digital images of Geometric Morphometric (GM) landmarks (fig. 2), following Armbruster (2012), were created using TpsUtil 1.70 (Rohlf, 2015) and TpsDig2 (Rohlf, 2015).

Twenty-six morphometric measurements and 18 meristic counts (tables 1 and 2) were taken following Tshibwabwa and Teugels (1995) and slightly modified after Tshibwabwa et al. (2006), Moritz (2007), Moritz and Neumann (2017), and Armbruster (2012). Measurements were made point to point, except for the caudal peduncle and postorbital length which were measured as horizontal distances, using the linear measurement tool in TpsDig2 and digital calipers, whereas scale counts were made under a stereomicroscope. Body depth was measured as the vertical distance from the posterior insertion of the dorsal fin to the ventrum. Radiograph images were used to count the total number of vertebrae, pleural ribs, simple and branched dorsal and anal-fin rays, procurrent and principal caudal-fin rays. In contrast to Tshibwabwa et al. (2006) and Tshibwabwa and Teugels (1995), all vertebrae possessing a hemal spine were counted as caudal vertebrae whereas those with ribs and with hemal arches but lacking hemal spines were counted as abdominal vertebrae (Aguirre et al., 2014). Circumpeduncular scales were counted at the narrowest point around the caudal peduncle (Reid, 1985). Weberian vertebrae and the preural centrum were excluded from all counts. Traditional morphometric and meristic data were analyzed separately in R (R Core Team, 2013) using principal component analysis as implemented in the package FactoMineR (Lê et al., 2008). Morphometric data were analyzed as log-transformed proportions of SL with measurements of fin lengths excluded (due to fin damage). Invariant meristic counts

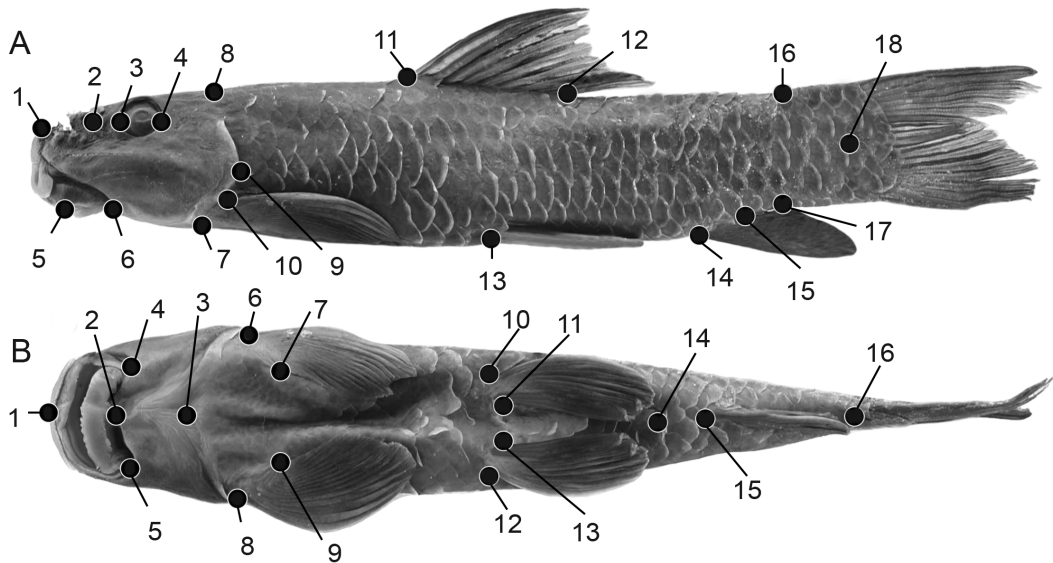


FIGURE 2. Homologous landmarks used in geometric morphometric analyses (following Armbruster, 2012): **A.** lateral and **B.** ventral views.

(simple dorsal-fin rays, principal caudal-fin rays, simple pelvic-fin rays, branched pelvic-fin rays, and anal-fin rays) were removed from subsequent analyses.

A minimum of five representatives of each described species were CT-scanned at the AMNH's Microscopy and Imaging Facility (MIF), using either the nanofocus (180 kV/20 W) or the microfocus (240 kV/320 W) tubes of a Phoenix V|tome|XS240 microCT scanner (General Electric, Fairfield, CT) depending on specimen size. Specimens were scanned with a diamond target at resolutions varying between 18.1 and 64.02 μm and a beam energy between 120–140 kV and 90–110 μA depending on specimen density. A total of 2500 projections per specimen were collected for 400 ms each and averaged 3–4 times to improve signal-to-noise ratios. Image reconstructions were conducted using the Phoenix datosjx (General Electric, Wunstorf, Germany) software and imported in Volume Graphics Studio Max 3.5.1 (Volume Graphics, Heidelberg, Germany) for segmentation and visualization. Segmented anatomical features were imaged in different views, with scale in Volume Graphics Studio Max 3.5.1 and imported in TpsDig2 for linear measurement.

RESULTS

PHYLOGENETIC RELATIONSHIPS: Details of phylogenetic analyses and the resultant maximum-likelihood phylogram have been published and discussed in Liyandja et al. (2022). *Labeo mbimbii* (as *Labeo* sp. 'mbimbii') and *L. manasseae* (as *Labeo* sp. 'Lulua') are resolved as members of a large, well-supported subclade of the *L. forskalli* group (subclade K of Liyandja et al., 2022: fig. 4), restricted almost entirely in geographical distribution to the Congo Basin, but

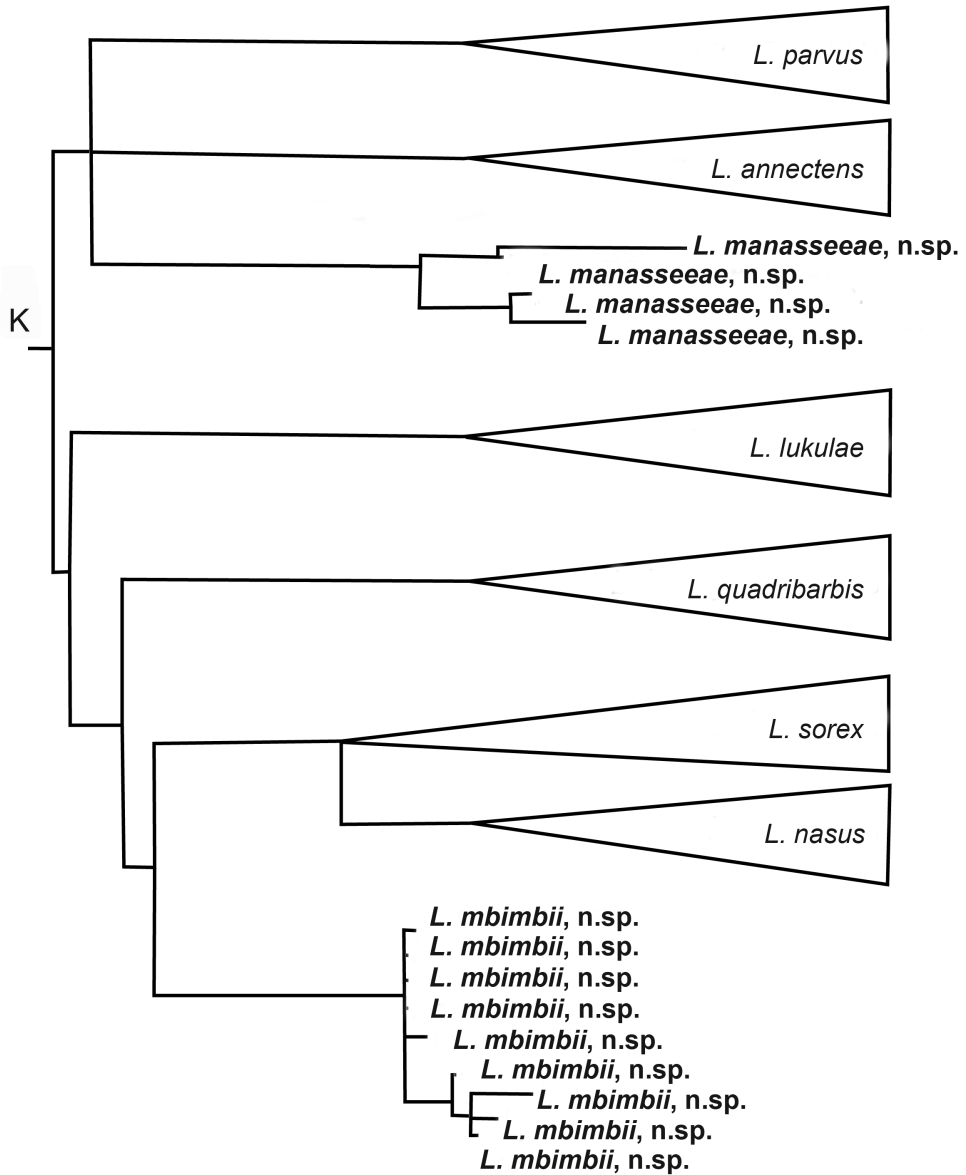


FIGURE 3. Simplified phylogram of subclade K modified after Liyandja et al. (2022) showing placement of *L. mbimbii*, n. sp., and *L. manasseeae*, n. sp. (in bold).

including two species (*L. annectens* and *L. lukulae*) from the southern portion of the adjacent Lower Guinean ecoregion (Southern West Coastal Equatorial ecoregion of Thieme et al., 2005). Here, for ease of reference, we provide a simplified figure of subclade K indicating the phylogenetic placement of the two new species in relation to described species (fig. 3). While the study of Liyandja et al. (2022) was based on a limited molecular dataset (concatenated CO1 and RAG1 loci, 2023 bp), preliminary analysis of a genome-wide marker set (2600+ UCE loci, >2,200,000 bp) with increased taxon sampling, supports a similar topology and corroborates the monophyly of each species (Liyandja et al., in prep.).

As indicated in figure 3, *L. mbimbii*, n. sp., is sister to the *L. sorex*–*L. nasus* subclade, while *Labeo manasseeae*, n. sp., belongs to the *L. parvus* subclade and, despite superficial resemblance, neither taxon is phylogenetically closely related to the poorly known Lulua River endemic, *L. luluae* (Liyandja et al., 2022; see Discussion).

MERISTICS: After the removal of invariant counts, two principal component analyses (PCAs) were performed on the remaining counts. The first was performed on all species for 13 meristic counts while the second was performed on 12 meristic counts including only those species that were overlapping with *L. manasseeae*, n. sp., in the first PCA. In that analysis, 79.25% of meristic variation is explained by the first four principal components with PC1 and PC2 accounting respectively for 33.7% and 22.9% of variation in the data. Differences in scale counts contributed most to the factor loadings of PC1, with the number of scales between the lateral line and the dorsal fin having the highest influence (17.8%), whereas differences in the number of abdominal vertebrae (26.9%), pleural ribs (21.2%), total vertebrae (7.2%), and procurrent dorsal-fin rays (17.2%) contributed most to the loadings of PC2. PC1 divides these species into two groups: *L. annectens*, *L. dhonti*, and *L. lukulae* with higher total lateral-line scale counts, and higher counts between the lateral line and dorsal-fin origin (35 or more and 4.5–5.5) versus *L. luluae*, *L. manasseeae*, n. sp., *L. mbimbii*, n. sp., *L. parvus*, *L. quadribarbis*, *L. simpsoni* with fewer (35 or less and 4–4.5) (fig. 4A). PC2 divides these species in two groups as well, species (*L. annectens*, *L. dhonti*, and *L. mbimbii*, n. sp.) with higher abdominal vertebrae counts (16–17) versus those (*L. lukulae*, *L. luluae*, *L. manasseeae*, n. sp., *L. parvus*, *L. quadribarbis*, and *L. simpsoni*) with lower counts (14–15). In the scatter plot of these two principal components *L. mbimbii*, n. sp., is clearly distinguished from the remaining species while *L. manasseeae*, n. sp., overlaps with *L. parvus*, *L. quadribarbis*, *L. simpsoni*, and *L. luluae*. In the second analysis the first four principal components accounted for 62.7% of the data variation; however, this analysis failed to separate these species from *L. manasseeae*, n. sp. (fig. 4B), suggesting that meristic features alone are unable to discriminate among these species.

MORPHOMETRICS: A PCA was performed on 17 morphometric measurements after removal of fin measurements (due to fin damage) (fig. 4C). The first five principal components account for 71.1% of total variation with PC1, PC2, and PC3 accounting respectively for 26%, 15.1%, and 12.4% of variation. Differences in the interpectoral width (14.6%), prepelvic length (12%), vent–anal–fin distance (10.3%), predorsal length (9.9%), head length (7.5%), and caudal peduncle depth (6.8%) contributed the most to the factor loadings of PC1, whereas differences in the orbital length (19.5%), prepectoral length (15.4%), head length (14.8%), interorbital

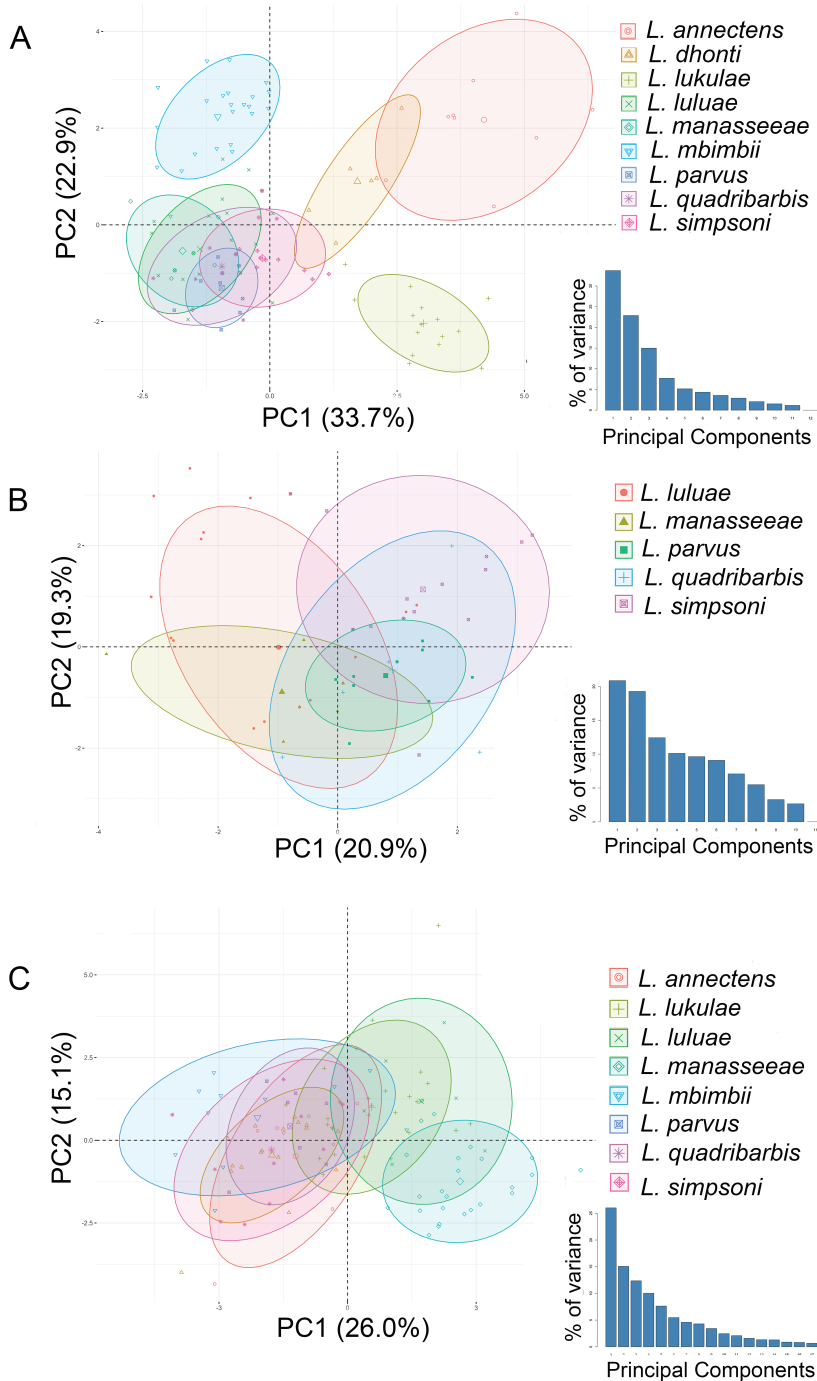


FIGURE 4. **A.** Scatterplot of PC2 against PC1 (PCA of 13 meristic counts for 120 specimens representative of 9 species). **B.** Scatterplot of PC2 against PC1 (PCA of 12 meristic counts for 44 specimens representative of the five species overlapping with *L. manasseeae* in A). **C.** Scatterplot of PC2 against PC1 (log-transformed matrix, 12 morphometric measurements, for 114 specimens representative of 8 species).

width (10.2%), postorbital head length (8.1%), and caudal peduncle length (7.8%) contributed the most in the loadings of PC2. PC1 divided these species into two main groups: *L. mbimbii*, n. sp., *L. manasseeae*, n. sp., and *L. luluae* with shorter vent–anal-fin distance (3.8%–6.9% SL) versus *L. lukulae*, *L. parvus*, *L. quadribarbis*, and *L. simpsoni* with longer vent-anal fin distance (7.1%–11.4%SL). Although the scatter plot of PC1 vs PC2 (fig. 4C) indicates separation there is still some overlap.

***Labeo mbimbii*, new species**

Figures 5, 6; table 1

Labeo cf. *lukulae*: Mbimbi et al., 2021

Labeo sp. ‘mbimbii’: Liyandja et al., 2022

HOLOTYPE: AMNH 277862 (AMCC 249232, CT), 91.5 mm SL, main channel of the Lulua River over rocks at Dipumu Rapids, about 47 km downstream of Katende Dam, Kasai Central Province, D.R. Congo, 05°56′12.4″S, 022°20′22.1″E, J.J. Mbimbi and T. Liyandja, September 2014.

PARATYPES: AMNH 253456 (2, CT), 94.2–104.2 mm SL, main channel of the Lulua River over rocks and rapids at Dijiba, about 19 km downstream of Katende dam, Kasai Central Province, D.R.C., 06°10′21.8″S, 022°27′07.7″E, J.J. Mbimbi, July 2010; AMNH 269102 (2), 62.3–70.4 mm SL, main channel of the Lulua River over rocks at about 155 km in straight line upstream of Katende Dam, Kasai Central Province, D.R.C., 07°44′21.7″S, 022°36′39.6″E, J.J. Mbimbi and T. Liyandja, September 2014; AMNH 277863 (4, 2 CT), 81.5–93.8 mm SL, same locality as holotype, J.J. Mbimbi and T. Liyandja, September 2014; AMNH 277864 (6, 1 CT), 62.0–71.6 mm SL, main channel of the Lulua River over rocks at Nsanga Nyembo Rapids, about 45.5 km in a straight line downstream of Katende Dam, Kasai Central Province, D.R.C., 05°56′53.4″S, 022°20′29.4″E, J.J. Mbimbi, July 2008; AMNH 277865 (2), 81.3–84.5 mm SL, main channel of the Lulua River over rocks downstream Nsanga Nyembo, about 47 km in a straight line downstream of Katende Dam, Kasai Central Province, D.R.C., 05°55′55.8″S, 022°20′27.6″E, J.J. Mbimbi, July 2008; AMNH 277866 (3), 78.09–83.37 mm SL, same locality as AMNH 277864, J.J. Mbimbi, July 2008; ANSP 208760 (1), 90.05 mm SL, main channel of Lulua River in rocky habitat at about 2 km upstream of Dipumu Rapids, Kasai Central Province, D.R.C., 05°57′17.8″S, 022°20′43.3″E, J.J. Mbimbi and T. Liyandja, September 2014; ANSP 208761 (1), 80.6 mm SL, main channel of the Lulua River over rocks at Katende Rapids, Kasai Central Province, D.R.C., 06°20′37.2″S, 022°27′1.3″E, J.J. Mbimbi, January 2009; MRAC 2023.001.P.0001–0002 (2), 85.69–92.68 mm SL, same locality as holotype, J.J. Mbimbi and T. Liyandja, September 2014; ZSM 48369 (2), 94.67–103.6 mm SL, same locality as holotype, J.J. Mbimbi and T. Liyandja, September 2014.

ADDITIONAL NONTYPE MATERIAL: AMNH 269104 (11), 53.48–82.13 mm SL, same locality as holotype, J.J. Mbimbi and T. Liyandja, September 2014.

DIFFERENTIAL DIAGNOSIS: While no unambiguous morphological autapomorphies have been located to diagnose *Labeo mbimbii*, the species is distinguished from all central African

TABLE 1. *Labeo mbimbii*, n. sp., Morphometric measurements and meristic data for the holotype and 25 paratypes.

	Holotype	Holotype + Paratypes		
		Max	Min	Mean±SD
Morphometric measurements				
Standard length (SL) (mm)	91.5	104.2	62.0	
Body depth (mm)	16.4	19.3	11.1	15.5±2.2
Head length (mm)	24.2	27.8	16.1	21.8±3.0
Caudal peduncle length (mm)	10.2	13.4	7.3	10.3±1.4
% SL				
Body depth (BD)	18	19.8	17.8	18.8±0.5
Caudal peduncle depth (CPD)	14.6	14.9	13.0	14.4±0.5
Head length (HL)	26.4	28.7	25.1	26.4±0.8
Predorsal length (PDL)	47.1	50.2	46.2	47.9±1.0
Preanal length (PAL)	82.4	84.7	78.4	81.4±1.8
Prepelvic length (PVL)	56.5	58.3	53.8	56.4±1.2
Prepectoral length (PPL)	27	28	24.3	26.2±1.1
Dorsal-fin base (DFL)	21.1	26.5	19.2	22.0±1.4
Dorsal-fin length (DRL)	24.9	26.9	22.6	24.8±1.2
Pectoral-fin length (PL)	22	23.5	20.0	22.3±0.9
Pelvic-fin length (VL)	20	21.4	18.1	19.8±0.8
Anal-fin base (AL)	8.6	8.6	7.1	7.8±0.3
Anal-fin length (ARL)	18.8	21.4	18.4	19.7±1.0
Vent–anal-fin length (VAL)	5.6	6.7	4.1	5.7±0.7
Caudal peduncle length (CPL)	11.1	13.9	11.1	12.5±0.6
% HL				
Snout length (SnL)	52.3	54.7	45.9	51.1±2.2
Interorbital width (IOW)	38.4	43.6	32.5	39.0±2.3
Internarial width (INW)	31.1	31.6	25.1	28.9±1.6
Bony orbital diameter (ED)	25.5	28.3	21.5	24.6±1.4
Postorbital length (POL)	25.6	33.8	24.9	27.8±2.0
%BD				
Interpectoral width (IPW)	111.1	117.8	100.2	106.1±4.7
%CPL				
Caudal peduncle depth (CPD)	131.3	131.3	101.0	115.9±7.3
Meristic counts				
		Max	Min	Mode
Simple dorsal-fin rays	3	3	3	3
Branched dorsal-fin rays	9	10	9	10

TABLE 1 *continued*

	Holotype	Holotype + Paratypes		
		Max	Min	Mode
Scales in lateral line	31+3	32+3	31+3	31+3
Scale rows between lateral line and dorsal fin	4	4.5	4	4
Scale rows between lateral line and pelvic fin	3	3.5	3	3
Circumpeduncular scales	12	12	12	12
Predorsal scales	9	10	9	9
Principal caudal-fin rays	19	19	19	19
Upper procurrent caudal-fin rays	9	9	8	8
Lower procurrent caudal-fin rays	7	8	7	7
Simple pelvic-fin rays	1	1	1	1
Branched pelvic-fin rays	8	8	8	8
Simple anal-fin rays	3	3	3	3
Branched anal-fin rays	5	5	5	5
Total vertebrae	29	29	28	29
Abdominal vertebra	16	17	16	16
Caudal vertebra	13	13	12	13
Pleural ribs	13	14	12	13

L. forskalii group congeners except *L. dhonti*, *L. lukulae*, *L. luluae*, *L. manasseeae*, n. sp., *L. parvus*, *L. quadribarbis*, and *L. simpsoni* in the possession of 28–29 vertebrae (vs. 30 or more), and from all of these species in the possession of 5 (vs. 4) predorsal vertebrae, 4 (vs. 3) well-developed supraneural bones between the neural spines of the predorsal vertebrae, and generally 3 (vs. 4) unbranched dorsal-fin rays. It is further distinguished from *L. manasseeae*, n. sp., in the possession of a snout with a deep ethmoid furrow and well-developed fleshy appendage vs. a snout with a shallow ethmoid furrow and weakly developed fleshy appendage, and a robust, deep-keeled, thick-necked urohyal bone (vs. gracile, shallow keeled with narrow neck).

DESCRIPTION: Based on holotype and 25 paratypes. General appearance as in figure 5, proportional measurements and meristic counts in table 1. Small-bodied species, maximum observed size 104.2 mm SL (AMNH 253456), elongate, cylindrical, somewhat dorsoventrally compressed (BD 17.8%–19.8% SL). Genital opening situated well in advance of anal-fin origin, vent–anal-fin distance 4.1%–6.7% SL. Head moderately large, with slightly convex or flattened interorbital space. Snout broad and truncate, ethmoid furrow deep, well-developed fleshy appendage with few (five to eight, generally five) large tubercles. Eyes large, dorsolaterally positioned, not visible in ventral view. Mouth large, inferior, lips plicate, anterior barbels absent, posterior barbels small, deeply embedded in lip fold, not externally visible.

Dorsal fin, iii 9 or 10 rays, margin slightly concave, inserted a little in front of midbody (predorsal length 46.2%–50.2% SL), anal fin, iii 5 rays. Caudal fin emarginate, 8–9 upper, 7–8

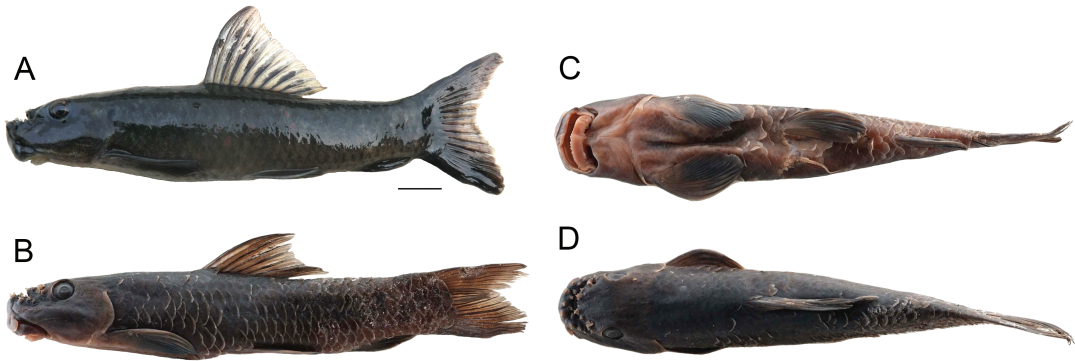


FIGURE 5. *Labeo mbimbii*, n. sp. Holotype (AMNH 277862, AMCC 249232) in **A.** lateral view, immediately postmortem; **B.** in preservation, lateral view; **C.** ventral view; and **D.** dorsal view. Scale bar = 1 cm.

lower procurrent rays, 19 principal rays. Pectoral fins broad, inserted lateroventrally, interpectoral width 100.2%–117.8% BD. Pelvic fins, 8, slightly shorter than pectorals.

Scales cycloid, 31(21)–32(5) in lateral line to hypural joint; 4–4.5 between lateral line and dorsal-fin origin; 3–3.5 between lateral line and pelvic-fin origin; 12 circumpeduncular. Total vertebral count (exclusive of 4 Weberian centra and terminal preural centrum), 28–29 (mode 29), comprised of 16–17 (mode 16) abdominal and 12–13 (mode 13) caudal centra.

Some additional osteological features variable among African *Labeo* are presented in figure 6. The Weberian apparatus of *L. mbimbii* is relatively massive (fig. 6A), with the anterior Weberian supraneural (supraneural 3 following the nomenclature of Bird and Hernandez, 2007) robust, 1.2× longer than tall, and in direct contact with the supraoccipital. No supraneural between the neural spine of the fourth Weberian centrum and the neural spine of the first predorsal centrum. Four supraneural bones anterior to the neural spines of predorsal centra 2–5. Five predorsal vertebrae. Urohyal (fig. 6B) robust, thick-necked, with a deep keel. Infra-orbital series (fig. 6C) consists of an elongate first infraorbital (lachrymal) and four additional elements, none of which are ventrally expanded or in contact with the preopercle.

COLORATION: Immediately postmortem (fig. 5A) coloration varies from black to dark gray or brown above, pale brown to whitish below, no dark lateral band visible either in adults or juveniles. Preserved specimens (fig. 5B–D) are dark brown above and paler brown below. A dark lateral band is visible in preserved juveniles.

DISTRIBUTION: A Lulua River endemic, known from the main channel of the lower and middle Lulua basin (fig. 1).

BIOLOGY AND ECOLOGY: All specimens of *L. mbimbii* have been collected in rapids along the Lulua River main channel over rocky substrates. These observations, combined with a dorsoventrally compressed body shape, suggest that *L. mbimbii* is adapted to rapid, rocky main-channel habitats. The waters where specimens have been collected are slightly acidic (pH 5.5–6.5), with low conductivity (2–5 $\mu\text{S}/\text{cm}^2$) and low concentrations of dissolved solids (TDS 4–10 ppm).

ETYMOLOGY: *Labeo mbimbii* is named for Prof. José Justin Mbimbi Mayi Munene (JJMMM) of the Biology Department, College of Sciences, University of Kinshasa. JJMMM is the lead

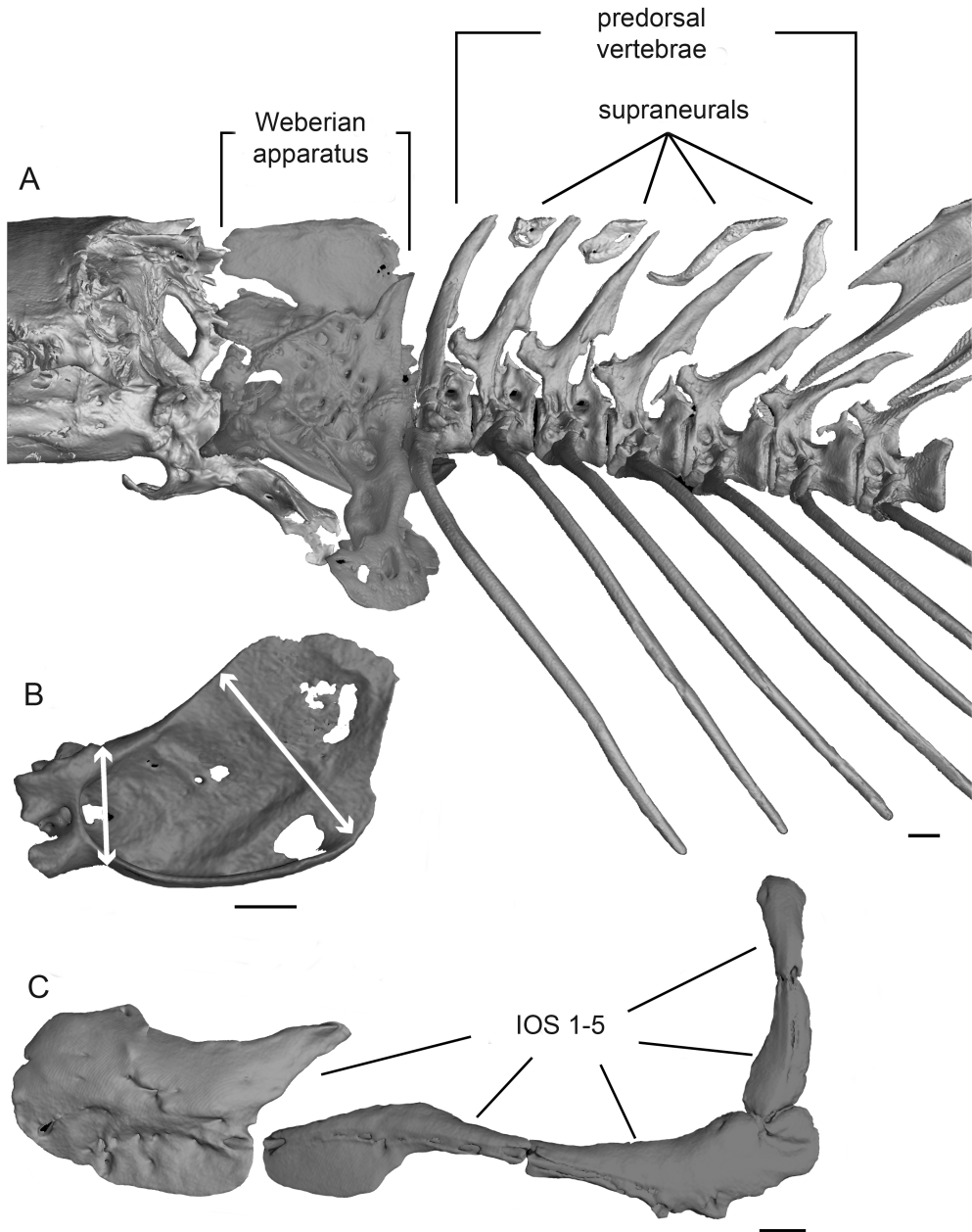


FIGURE 6. *Labeo mbimbii*, n. sp. Holotype (AMNH 277862): CT scan renderings of A. posterior neurocranium, Weberian apparatus and proximal axial elements; B. isolated urohyal bone; and C. infraorbital series. Scale bars = 1 mm

investigator and PI of the Lulua Project that has resulted in the deposition at the AMNH and the University of Kinshasa, of more than 5000 specimens representing over 200 species, including those described in the present paper. We dedicate this species to his outstanding work and commitment to biodiscovery and conservation in the Kasai basin.

Labeo manasseeae, new species

Figures 7, 8; table 2

Labeo sp. nov.: Mbimbi et al., 2021

Labeo sp. 'Lulua': Liyandja et al., 2022

HOLOTYPE: AMNH 269110 (AMCC 249240, CT), 121.2 mm SL, main channel of the Lulua River over rocks at Sandoa (Sanduwa), 0.05 km downstream of Sandoa Bridge, Lualaba Province, D.R.C., 09°41'37.2"S, 022°51'30"E, J.J. Mbimbi and T. Liyandja, September 2014.

PARATYPES: AMNH 269103 (AMCC 249230, CT), 97.3 mm SL, main channel of the Lulua River in rocky and rapids habitat about 0.35 km downstream of crossing point on road to Kapanga, Lualaba Province, D.R.C., 08°16'04.3"S, 022°35'50.2"E, J.J. Mbimbi and T. Liyandja, September 2014; AMNH 277861 (AMCC 249238–9, 2, 2 CT), 52.88–70.46 mm SL, collected with AMNH 269103; ZSM 48370 (2, 1 CT), 50.23–74.47 mm SL, Lukushi River (tributary of Lulua) at Mukanda rapids, Lualaba Province, D.R.C., 10°30'25.4"S, 23°23' 33.8"E, E. Vreven et al., August 2012.

ADDITIONAL NONTYPE MATERIAL: AMNH 247858, 1, 116.4 mm SL, main channel of the Lulua River over rocks at Ntumba Shambuyi Rapids located 2.23 km downstream of Dipumu Rapids, Kasai Central Province, D.R.C., J.J. Mbimbi, July 2008.

DIFFERENTIAL DIAGNOSIS: While no unambiguous morphological autapomorphies have been located to diagnose *Labeo manasseeae* the species is distinguished from all central African *L. forskalii* group congeners except *L. dhonti*, *L. lukulae*, *L. luluae*, *L. mbimbii*, *L. parvus*, *L. quadribarbis*, and *L. simpsoni* in the possession of 28 vertebrae (vs. 30 or more). *Labeo manasseeae* is distinguished from *L. lukulae*, *L. luluae*, and *L. quadribarbis* by a larger interpectoral width (94.7%–107.9% vs. 66.7%–92.8% BD), from *L. parvus*, *L. quadribarbis*, and *L. simpsoni* by a shorter vent–anal–fin distance (5.0%–6.9% vs. 11.4%–7.1% SL), and from *L. dhonti* and *L. lukulae* in the possession of 30–31 (vs. 35–36) pored lateral-line scales. It is distinguished from *L. mbimbii* in the possession of 3 fully developed supraneural bones (vs. 4), 4 predorsal vertebrae (vs. 5), a pointed snout with a shallow ethmoid furrow and weakly developed fleshy appendage versus a truncate snout with a deep ethmoid furrow and well-developed fleshy appendage, and a gracile, narrow-necked, shallow-keeled (vs. robust, thick-necked, and deep-keeled) urohyal bone.

DESCRIPTION: Based on the holotype and five paratypes. General appearance as in figure 7, proportional measurements and meristic counts in table 2. Small-bodied species, maximum observed size 121.2 mm SL (holotype), elongate, cylindrical, somewhat dorsoventrally compressed (BD 16.1%–19.2% SL). Genital opening situated well in advance of anal-fin origin, vent–

TABLE 2. *Labeo manasseae*, n. sp., morphometric measurements and meristic data for the holotype and five paratypes.

	Holotype	Holotype + Paratypes		
		Max	Min	Mean±SD
Morphometric measurements				
Standard length (mm)	121.2	121.2	50.2	
Head length (mm)	31.5	31.5	14.3	22.3±6.8
Body depth (mm)	22.2	22.2	8.9	15.0±5.4
Caudal peduncle length (mm)	15.9	15.9	6.2	10.4±4.9
% SL				
Body depth (BD)	18.3	19.2	16.1	17.5±1.2
Caudal peduncle depth (CPD)	13.7	14.7	12.1	13.2±1.0
Head length (HL)	26.0	28.9	26.0	26.7±1.0
Predorsal length (PDL)	44.8	48	44.8	46.5±1.1
Preanal length (PAL)	81.6	81.7	79.8	81.2±0.7
Prepelvic length (PVL)	56.2	59.6	56.2	57.2±1.2
Prepectoral length (PPL)	25.7	29.5	25.7	27.3±1.3
Dorsal-fin base (DFL)	20.0	22.7	19.6	20.8±1.2
Dorsal-fin length (DRL)	24.2	27.9	23.7	26.2±1.8
Pectoral-fin length (PL)	20.5	21.8	18.9	20.7±1.0
Pelvic-fin length (VL)	17.9	19.1	16.9	18.3±0.8
Anal-fin base (AL)	7.5	8.5	7.3	7.7±0.4
Anal-fin length (ARL)	18.8	19.2	16.9	18.5±0.8
Vent–anal-fin length (VAL)	6.4	6.9	5.0	6.2±0.6
Caudal peduncle length (CPL)	13.1	13.4	11.7	12.5±0.6
% HL				
Snout length (SnL)	52.1	51.5	45.5	48.5±2.4
Interorbital width (IOW)	36.2	39.1	33.3	35.6±2.5
Internarial width (INW)	27.5	30.1	23.7	26.4±2.7
Bony orbital diameter (ED)	24.3	28.2	19.8	24.2±2.9
Postorbital length (POL)	27.7	33.9	28.0	30.8±1.9
%BD				
Interpectoral width (IPW)	101.3	107.9	94.7	101.3±4.3
%CPL				
Caudal peduncle depth (CPD)	104.8	121.4	98.5	106.6±8.8
Meristic counts				
		Max	Min	Mode
Simple dorsal-fin rays	4	4	4	4
Branched dorsal-fin rays	10	10	10	10

TABLE 2 *continued*

	Holotype	Holotype + Paratypes		
		Max	Min	Mode
Scales in lateral line	31+3	31+3	30+3	31+3
Scale rows between lateral line and dorsal-fin origin	4	4	4	4
Scale rows between lateral line and pelvic-fin origin	3	3	3	3
Circumpeduncular scales	12	13	12	12
Predorsal scales	9	10	8	9
Principal caudal-fin rays	19	19	19	19
Upper procurrent caudal-fin rays	8	8	8	8
Lower procurrent caudal-fin rays	7	7	6	6
Simple pelvic-fin rays	1	1	1	1
branched pelvic-fin rays	8	8	8	8
Simple anal-fin rays	3	3	3	3
Branched anal-fin rays	5	5	5	5
Total vertebrae	28	28	28	28
Abdominal vertebra	15	16	15	15
Caudal vertebra	13	13	12	13
Pleural ribs	12	13	12	12

anal-fin distance 5.0%–6.9% SL. Head moderately large, with slightly convex interorbital space. Snout narrow and pointed, ethmoid furrow shallow, weakly developed fleshy appendage bearing 8 or more small tubercles. Eyes large, dorsolaterally positioned, not visible in ventral view. Mouth relatively small, inferior, lips plicate, anterior barbels small (absent in large specimens), posterior barbels small, deeply embedded in lip fold, externally visible in small specimens.

Dorsal fin, iv10 rays, margin slightly concave, inserted just anterior to midbody (predorsal length 44.8%–48.0% SL), anal fin iii5 rays. Caudal fin strongly emarginate, 8 upper, 6–7 lower procurrent rays, 19 principal rays. Pectoral fins broad, inserted lateroventrally, interpectoral width 94.7%–107.9% BD. Pelvic fins, i8, slightly shorter than pectorals.

Scales cycloid, 30–31 in lateral line to hypural joint; 4 between lateral line and dorsal-fin origin; 3 between lateral line and pelvic-fin origin; 12 circumpeduncular. Total vertebral count (exclusive of 4 Weberian centra and the terminal preural centrum), 28, comprised of 15–16 (mode 15) abdominal and 12–13 (mode 13) caudal centra.

The Weberian apparatus of *L. manasseae* is relatively massive (fig. 8A), with anterior Weberian supraneural 3 relatively gracile, 1.3× longer than tall, and in direct contact with the supraoccipital. No supraneural between the neural spine of the fourth Weberian centrum and the neural spine of the first predorsal centrum. Three fully developed supraneural bones anterior to the neural spines of predorsal centra 2–4 (a vestigial fourth supraneural bone is present in the holotype, but absent

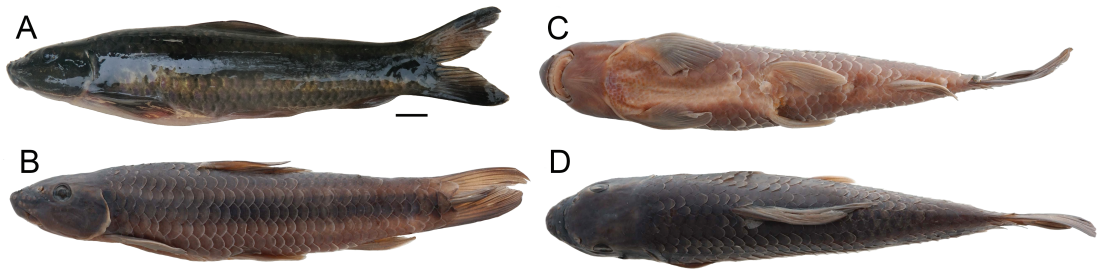


FIGURE 7. *Labeo manasseeae*, n. sp. Holotype (AMNH 269110, AMCC 249240): **A.** immediately postmortem; **B.** in preservation, lateral view; **C.** ventral view; and **D.** dorsal view. Scale bar = 1 cm

in all other specimens). Four predorsal vertebrae. Urohyal (fig. 8B) is gracile, thin necked, with a shallow keel. Infraorbital series (fig. 8C) consists of an elongated first infraorbital (lachrymal) and four additional elements, none of which are ventrally expanded or in contact with the preopercle.

COLORATION: Immediately postmortem (fig. 7A) coloration varies from brown to dark brown or black above, pale brown to cream below, a dark lateral band is barely visible at any size. Preserved specimens (fig. 7B–D) are dark brown above and brown below, and dark lateral band is visible in most specimens.

DISTRIBUTION: A Lulua River endemic, *Labeo manasseeae* is known mainly from the middle basin, with single records from the lower and upper basins (fig. 1). However, due to inaccessibility the upper Lulua has been poorly sampled (Mbimbi et al., 2021) and it is likely that additional collecting efforts will expand the range of this species.

BIOLOGY AND ECOLOGY: *Labeo manasseeae* has been collected in rocky, rapids habitats in the main channel of the middle Lulua, with one occurrence in a tributary of the upper basin. As for *L. mbimbii*, *L. manasseeae* appears to be adapted to rocky, rapids habitats of both the main channel and tributaries. The water in the main channel sites where *L. manasseeae* was collected is slightly acidic (pH 5.5–6.5), has low conductivity (2–5 $\mu\text{S}/\text{cm}^2$), and low concentration of dissolved solids (TDS 4–10 ppm).

ETYMOLOGY: Dedicated to Manassée W.E. Liyandja, the daughter of Tobit Liyandja. Manassée was born a few months prior to the expedition that led to the discovery of this new species and is an ongoing source of motivation for T.L.

DISCUSSION

Despite the extensive revisional work of Tshibwabwa (1997), species delimitation and identification among African *Labeo* remains challenging. Van Steenberge et al. (2016) suggested that one reason for the difficulty in correctly identifying species of *Labeo*, particularly in the Congo basin, is that many of the morphological characters traditionally used for species identification are subject to considerable allometric and geographic variation. Liyandja et al. (2022) concluded that in addition to these problems, pervasive convergent evolution in body form and pigmentation patterning among *L. forskalii* group species has resulted in

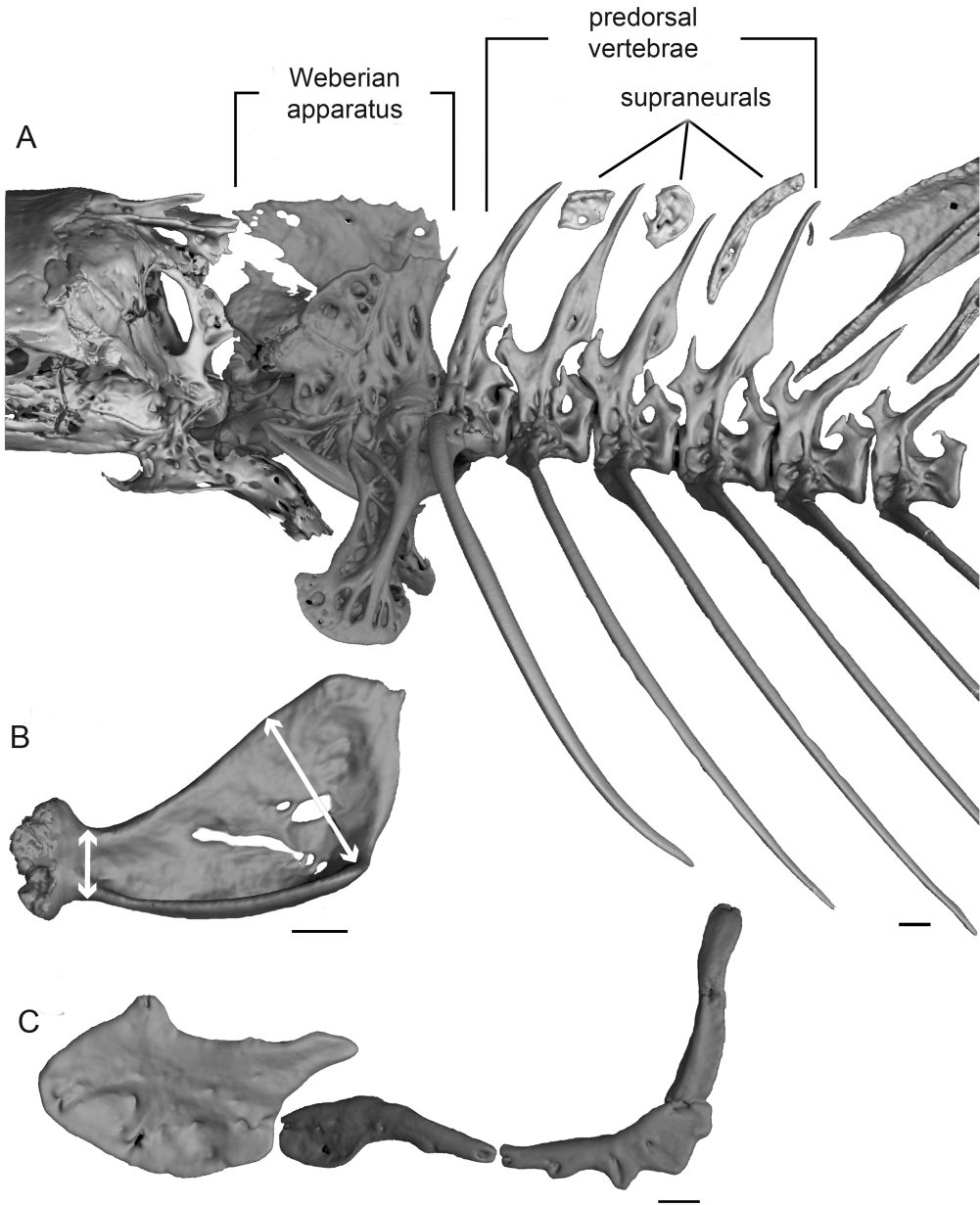


FIGURE 8. *Labeo manasseae*, n. sp. Holotype (AMNH 269110): CT scan renderings of **A.** posterior neurocranium, Weberian apparatus and proximal axial elements; **B.** isolated urohyal bone; and **C.** infraorbital series. Scale bars = 1 mm.



FIGURE 9. **A.** *Labeo luluae*, holotype (ANSP 51740). **B.** *Labeo lugubris*, holotype (AMNH 12334). Scale bars = 1 cm.

similar ecomorphs exhibited by distantly related species that overlap in most traditionally employed meristic and morphometric measures. Recent genetic investigations have identified well-supported monophyletic species and species groups, but also have revealed high levels of cryptic diversity with numerous previously unrecognized lineages and putative new species (Lowenstein et al., 2011; Liyandja et al., 2022). Despite strong molecular support for the recognition of many of these entities as distinct species (Liyandja et al., 2022; e.g., fig. 4), diagnostic morphological features are frustratingly elusive. Yet formal taxonomic and nomenclatural recognition of such morphologically cryptic species is of central importance for accurate biodiversity assessments, sustainable fisheries management, and regional conservation efforts. Here we provide differential diagnoses for two new species relying on combinations of meristic, morphometric measures, and osteological features, with the latter unfortunately not visible from external examination. While we acknowledge the problematic nature of such differential diagnoses for field identification, we believe that these diagnoses will at least aid in the correct identification of museum-held specimens, and facilitate a more accurate assessment of biological diversity in future studies.

Recently, Mbimbi et al. (2021) highlighted the exceptionally high diversity of the Lulua River ichthyofauna, suggesting that this large tributary in the Kasai ecoregion harbors one of the most species-rich fish communities in the entire Congo basin. Certainly, with the co-occurrence of an estimated 14 species, the Lulua basin is outstanding in terms of *Labeo* diversity, and unmatched as far as we can determine by any other region in the Congo basin or indeed elsewhere across the continent. Despite these high species numbers, prior to the present study, a single *Labeo* species was considered endemic to the Lulua River. That species is *Labeo luluae*, a taxon described by Fowler (1930) based on a single juvenile, now in poor preservation (ANSP 51740, 30.4 mm SL, fig. 9A) collected from the rapids of Katende (the site of a present-day hydroelectric plant) in the lower portion of the Lulua Basin. Tshibwabwa (1997) reported a second specimen that he identified as *L. luluae* from the Aruwimi River, at a site over 1000 km northwest of Katende in the Uele ecoregion. Although, we have been unable to examine that

specimen, from Tshibabwa's description and our own investigation of the holotype we conclude that the Aruwimi specimen is not conspecific with *L. luluae* and its assignment remains uncertain. However, based on detailed examination of the holotype and subsequent comparison of CO1 sequences we tentatively identify numerous additional specimens from the lower Lulua as *L. luluae* (see Comparative Materials Examined). However, as the preliminary phylogenetic analyses of Liyandja et al. (2022) recovered two divergent groups among these putative *L. luluae* samples, additional investigation of this potential complex will be necessary to determine whether these specimens represent a single or multiple Lulua River endemics; a necessary prerequisite for a formal taxonomic redescription of *L. luluae* (Liyandja et al., in prep.). Parenthetically, we note that *L. lugubris* described by Nichols and LaMonte (1933) for a single specimen from Luluabourg (Kananga) in the lower Lulua basin has been synonymized with *L. chariensis* (Reid, 1985; Tshibwabwa, 1997) a species originally described from the Chari River not the Congo. However, examination of the holotype (AMNH 12334, fig. 9B) suggests that *L. lugubris* is morphologically closely related to specimens assigned here to the *L. luluae* complex. We therefore consider the synonymy of *L. lugubris* with *L. chariensis* in error, however, final resolution of its correct placement must await further investigation of the *L. luluae* complex as a whole. Regardless, the holotype of *L. lugubris* can readily be distinguished from both of the new species described here by a longer vent–anal-fin distance (10.4 vs. 6.9–4.1% SL). Additionally, it differs from *L. mbimbii* by having fewer predorsal vertebrae (4 vs. 5), more small tubercles over the fleshy snout appendage, and the lack of a deep ethmoid furrow. *Labeo lugubris* is further distinguished from *L. manasseae* by total vertebral number (29 vs. 28), urohyal shape (robust vs. gracile), number of upper procurent caudal-fin rays (9 vs. 8), longer snout (65.6% vs. 45.5–51.5% HL), deeper caudal peduncle (140.0% vs. 98.5%–121.4% CPL), and smaller orbital diameter (15.1 vs. 19.8%–28.2% HL).

Regardless of the final resolution of the species composition of *L. luluae* and subsequent synonymy of *L. lugubris*, the current study brings the number of *Labeo* species endemic to this single basin minimally to three, and strengthens the proposal of Mbimbi et al. (2021) that the Lulua River may merit consideration as a separate ecoregion within the Kasai basin, and is one in urgent need of renewed conservation attention.

ACKNOWLEDGMENTS

This research was funded by the Axelrod Research Curatorship (MLJS) and a graduate fellowship from the Richard Gilder Graduate School of the American Museum of Natural History (TLDL). We are especially grateful to Thomas Vigliotta, Radford Arrindell, Chloe Lewis, Morgan Chase, and Lauren Audi for technical assistance to TLDL during the realization of this research. We also gratefully acknowledge Maxwell Bernt, Bruno Melo, and Naoko Kurata for their companionship and advice, with especial thanks to Bruno Melo for insightful input on an earlier version of this paper. We thank David Werneke and Jonathan W. Armbruster (AUM), Casey Dillman (CUMV), Brian Sidlauskas (OS), Dirk Neumann (ZSM), and Mark H. Sabaj (ANSP) for specimen loans, tissues gifts, and sharing pictures of type specimens.

REFERENCES

- Aguirre, W.E., K. Walker, and S. Gideon. 2014. Tinkering with the axial skeleton: vertebral number variation in ecologically divergent threespine stickleback populations. *Biological Journal of the Linnean Society* 113 (1): 204–219.
- Armbruster, J.W. 2012. Standardized measurements, landmarks, and meristic counts for cypriniform fishes. *Zootaxa* 3586: 8–16.
- Bennett, R.H., et al. 2016. Ethical considerations for field research on fishes. *Koedoe* 58 (1): 1–15.
- Bird, N.C., and L.P. Hernandez. 2007. Morphological variation in the Weberian apparatus of cypriniformes. *Journal of Morphology* 268 (9): 739–757.
- Fowler, H.W. 1930. The fresh-water fishes obtained by the Gray African Expedition: 1929. With notes on other species in the Academy Collection. *Proceedings of the Academy of Natural Sciences of Philadelphia* 82: 27–83.
- Fricke, R., W.N. Eschmeyer, and R. Van der Laan. 2022. Eschmeyer's catalog of fishes: genera, species, references. Online resource ([http:// researcharchive.calacademy.org/research/ichthyology/catalog/fishcatmain.asp](http://researcharchive.calacademy.org/research/ichthyology/catalog/fishcatmain.asp)), accessed 12.27.2022.
- Froese, R., and D. Pauly. 2022. FishBase. Online resource (<http://www.fishbase.org>), accessed 12.27.2022.
- Jenkins, J.A., et al. 2014. Guidelines for use of fishes in research, revised and expanded, 2014. *Fisheries* 39: 414–416.
- Lê, S., J. Josse, and F. Husson. 2008. FactoMineR: an R package for multivariate analysis. *Journal of Statistical Software* 25 (1): 1–18.
- Liyandja, T.L.D. 2018. Body shape evolution of African/Asian minnows of the genus *Labeo cuvier* 1817 (Cyprinidae, Labeonini) and variations in *Labeo parvus*. Master's thesis, Biological Sciences, Auburn University, Auburn, AL, 94 pp.
- Liyandja, T.L.D., J.W. Armbruster, M.O. Poopola, and M.L.J. Stiassny. 2022. Evolutionary convergence in body shape obscures taxonomic diversity in species of the African *Labeo forskalii* group: Case study of *L. parvus* Boulenger 1902 and *L. ogunensis* Boulenger 1910. *Journal of Fish Biology* 101: 898–913.
- Lowenstein, J.H., T.W. Osmundson, S. Becker, R. Hanner, and M.L.J. Stiassny. 2011. Incorporating DNA barcodes into a multi-year inventory of the fishes of the hyperdiverse Lower Congo River, with a multi-gene performance assessment of the genus *Labeo* as a case study. *Mitochondrial DNA* 22: 52–70.
- Mbimbi Mayi Munene, J.J., M.L.J. Stiassny, R.J.C. Monsembula Iyaba, and T.D.L. Liyandja. 2021. Fishes of the lower Lulua River (Kasai basin, central Africa): a continental hotspot of ichthyofaunal diversity under threat. *Diversity* 13 (8): 341.
- Moritz, T. 2007. Description of a new cyprinid species, *Labeo meroensis* n. sp. (Teleostei: Cyprinidae), from the River Nile. *Zootaxa* 1612 (1): 55–62.
- Moritz, T., and D. Neumann. 2017. Description of *Labeo latebra* (Cyprinidae) from the Nile River in Sudan. *Cybium* 41 (1): 025–033.
- Nguyen, L.-T., H.A. Schmidt, A. Von Haeseler, and B.Q. Minh. 2015. IQ-TREE: a fast and effective stochastic algorithm for estimating maximum-likelihood phylogenies. *Molecular Biology and Evolution* 32 (1): 268–274.
- R Core Team. 2013. R: A language and environment for statistical computing. Vienna: R Foundation for Statistical Computing. [Retrieved from <http://www.r-project.org/>]
- Reid, G.M. 1985. A revision of African species of *Labeo* (Pisces: Cyprinidae) and a re-definition of the genus. Braunschweig: Verlag von J. Cramer, 322 p.

- Roberts, E., H.A. Jelsma, and T. Hegna. 2015. Mesozoic sedimentary cover sequences of the Congo Basin in the Kasai Region, Democratic Republic of Congo. *In* M.J. De Wit et al. (editors), *Geology and resource potential of the Congo Basin*: 1–417. Berlin: Springer.
- Rohlf, F.J. 2015. The tps series of software. *Hystrix, the Italian Journal of Mammalogy* 26: 9–12.
- Ronquist, F., et al. 2012. MrBayes 3.2: Efficient bayesian phylogenetic inference and model choice across a large model space. *Systematic Biology* 61 (3): 539–542.
- Thieme, M.L., et al. 2005. *Freshwater ecoregions of Africa and Madagascar. A conservation assessment*. Washington DC: Island Press, 431 pp.
- Tshibwabwa, S.M. 1997. *Systématique des espèces africaines du genre Labeo (Teleostei; Cyprinide) dans les régions ichtyogéographiques de Basse-Guinée et du Congo*. Ph.D. dissertation, Biological Sciences, University of Namur, Namur, Belgium.
- Tshibwabwa, S.M., and G.G. Teugels. 1995. Contribution to the systematic revision of the African cyprinid fish genus *Labeo*: species from the lower Zaire River system. *Journal of Natural History* 29 (6): 1543–1579.
- Tshibwabwa, S.M., M.L.J. Stiassny, and R.C. Schelly. 2006. Description of a new species of *Labeo* (Teleostei: Cyprinidae) from the lower Congo River. *Zootaxa* 1224: 33–44.
- Van Steenberge, M., L. Gajdzik, A. Chilala, J. Snoeks, and E. Vreven. 2016. Don't judge a fish by its fins: species delineation of Congolese *Labeo* (Cyprinidae). *Zoologica Scripta* 46 (3): 264–274.

All issues of *Novitates* and *Bulletin* are available on the web (<https://digitallibrary.amnh.org/handle/2246/5>). Order printed copies on the web from:
<https://shop.amnh.org/books/scientific-publications.html>

or via standard mail from:

American Museum of Natural History—Scientific Publications
Central Park West at 79th Street
New York, NY 10024

Ⓒ This paper meets the requirements of ANSI/NISO Z39.48-1992 (permanence of paper).